

Electrical properties of fractal systems based on porous amorphous silicon

A. I. Yakimov, N. P. Stepina, A. V. Dvurechenskiĭ, L. A. Shcherbakova, and A. I. Nikiforov

Institute of Semiconductor Physics, Russian Academy of Sciences, Siberian Branch, 630090 Novosibirsk, Russia

(Submitted 22 December 1995)

Zh. Éksp. Teor. Fiz. **110**, 322–333 (July 1996)

The special features of conduction in porous amorphous silicon are investigated. Protracted non-Debye current relaxation (lasting tens of minutes) has been detected after a bias voltage is applied to the structure. It is shown, first, that the dynamic conductivity increases with the frequency of the electric field as $\omega^{0.94}$, and second, that the static conductivity varies with temperature as $\sigma(T) \propto \exp[-(T_0/T)^{0.45-0.46}]$. The entire body of experimental data is described well by a hopping conduction mechanism with a variable hopping length between superlocalized electron states in a fractal space of dimension $2 < D < 3$, which depends on the porosity of the material. The superlocalization exponent in the electronic wave functions on the fractals is found to be $\zeta = 1.9$, which attests to the validity of the interpretation of ζ as half of the fractal dimensionality of the random walks. © 1996 American Institute of Physics. [S1063-7761(96)02407-9]

1. INTRODUCTION

There has been growing interest in the investigation of the physical properties of silicon subjected to electrochemical etching in hydrofluoric acid, i.e., porous silicon, not only because this material is promising for applications in optoelectronic devices, but also because some unusual charge-transport laws, which reflect features of its structure, have been discovered in it. For example, a study of static hopping conduction in layers of porous amorphous silicon¹ obtained by ion implantation in crystalline Si followed by anodization has shown that the effective geometric dimension D of the current paths can have a fractional (fractal) value, which depends on the etching regime of the structures and, therefore, on the topological layout of the silicon skeleton. At low temperatures, at which the electron hopping distance becomes greater than the transverse diameter of the silicon columns, charge transport was one-dimensional and took place along chains of localized states separated by long pores perpendicular to the surface. A transition from the three-dimensional Mott regime of hopping conduction to the one-dimensional regime as the temperature is lowered has also been discovered and studied in detail in porous $a\text{-Si}_{1-x}\text{Mn}_x$.¹ Features of the frequency characteristics of the ac conductivity that attest to the fractal structure of the system have been obtained in crystalline porous silicon (c-PS).

The existence of self-similar properties of the porous silicon skeleton over a range of geometric scales has been pointed out in many experiments on the structural analysis of this material. They include the results of the small-angle scattering of x rays,^{3,4} neutron scattering,⁵ and high-resolution electron microscopy.⁶ Of course, the presence of the developed internal fractal surface characteristic of porous silicon should also influence the electrophysical properties of this substance.

Diffusion and transport in disordered media are often modeled by random walks over fractal structures. It is as-

sumed that a walk in space itself builds a fractal medium, selecting the sites visited according to certain probability laws. The track left by such walks forms a percolation cluster. One distinguishing feature of porous silicon is the fact that the space itself initially has self-similar structure inherent in the silicon skeleton formed after anodic etching. This has a very important consequence, which determines the details of charge transfer on the fractals. In fact, in contrast to the Anderson decay law $\Psi(r) \propto \exp[-r/a]$, the wave function of electrons localized on fractals decays more rapidly at large r (Ref. 7): $\Psi(r) \propto \exp[-(r/a_s)^\zeta]$, where the superlocalization exponent ζ is greater than unity and depends on the Euclidean dimensionality of the system. As a result, the microscopic rates of tunneling transitions of electrons on fractals are significantly lower than the rates in systems with Euclidean dimensionality, resulting in a considerable increase in resistance and slowing of various kinetic processes.

The present work is devoted to a detailed investigation of the features of hopping conduction in porous amorphous silicon obtained by spray deposition in an ultrahigh vacuum followed by electrolysis in a solution of HF. The main results of the work include the following:

(1) ac conductivity in the porous material increases with the frequency of the electric field as $\omega^{0.94}$ and is governed by subbarrier hopping of electrons in a medium with fractal dimension $D \approx 2.1-2.5$ and a superlocalization exponent $\zeta = 1.9$;

(2) after a voltage step is applied to the structure, non-Debye current relaxation lasting tens of minutes is observed, pointing out the partial nonergodicity of porous silicon as a Fermi glass;

(3) the temperature dependence of the static hopping conductivity of porous silicon with a porosity greater than 37% at high temperatures follows the law $\ln \sigma(T) \propto -(T_0/T)^{0.45-0.46}$, which attests to a fractal dimension D equal to 2.2–2.3 for the medium.

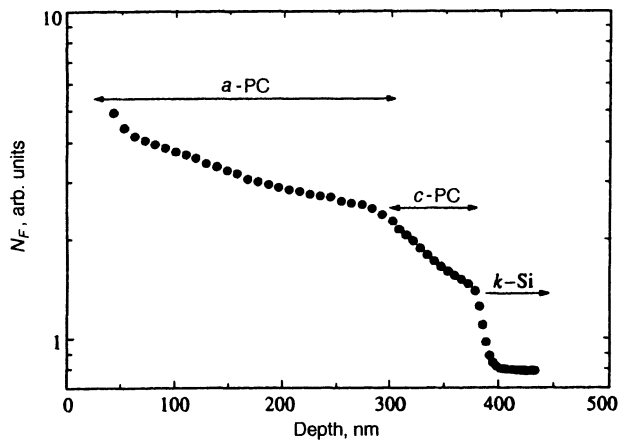


FIG. 1. Distribution of fluorine atoms obtained by SIMS in a structure subjected to electrolytic etching at a current density of 30 mA/cm² for 8 s.

2. EXPERIMENTAL SAMPLE

Films of amorphous silicon 300 nm thick were grown on a degenerate arsenic-doped silicon substrate with the (111) orientation in an ultrahigh-vacuum molecular-beam-epitaxy (MBE) system. The substrate temperature did not exceed 50 °C, despite the heating effect of the electron-beam evaporator. Immediately before the plates were inserted into the growth chamber, a thin layer of SiO₂ was chemically grown on the Si surface, and it was subsequently removed in the MBE chamber at 800 °C in a stream of silicon with a flux density equal to 10¹³ atoms/cm²·s, after which the 7×7 superstructure characteristic of a clean Si(111) surface was observed. The growth rate of amorphous Si did not exceed 1.5 Å/s, the structure was monitored directly in the chamber by high-energy electron diffraction, and the thickness of the *a*-Si layer was determined by a quartz thickness meter. The concentration of dangling bonds measured by electron spin resonance in similar *a*-Si layers deposited on glass was $N = 1.3 \times 10^{19}$ cm⁻³. Below we refer to amorphous silicon that has not been subjected to electrolysis as compact silicon.

Porous silicon was created by electrochemically etching the compact structures in a 42% solution of HF:H₂O:C₃H₇OH (1:1:2). To obtain structures with different density deficiencies, the anodic current density and the etching time were varied.

Figure 1 presents the depthwise distribution of fluorine atoms recorded by secondary-ion mass spectrometry (SIMS) for a sample anodized for 8 s at $j = 30$ mA/cm². Knowing the thickness of the amorphous layer, we were able to determine its porosity, which amounted to ~69%. Since fluorine atoms are immobilized on the pore surfaces, the depthwise variation of the specific surface and the porosity can be evaluated from the distribution of fluorine. It is seen that in *a*-Si the porosity decreases somewhat with depth. This is attributable to chemical dissolution of the surface layers. This effect is far more pronounced in the crystalline substrate, and it corresponds to the published data regarding the strong dissolution of *n*⁺-Si as a result of electrochemical etching.⁸

We established that the resistance of crystalline porous silicon exceeds the resistance of porous amorphous silicon.

TABLE I. Preparation conditions and characteristics of the structures.

| No. | j , mA/cm ² | t_{etch} , s | d , μm | ϵ | P , % |
|-----|--------------------------|-----------------------|----------|------------|---------|
| 1 | 0 | 0 | 0.30 | 12.1±0.1 | 0 |
| 2 | 15 | 4 | 0.041 | 6.2±0.1 | 37±2 |
| 3 | 15 | 6 | 0.063 | 4.3±0.1 | 52±3 |
| 4 | 15 | 9 | 0.093 | 4.2±0.1 | 54±3 |
| 5 | 15 | 12 | 0.125 | 4.0±0.1 | 54±3 |

Therefore, to eliminate the contribution from *c*-PS to the resistance of the structure, measurements of the transverse resistance were performed in samples obtained at lower current ($j = 15$ mA/cm²), in order that the thickness of the porous layer not exceed the thickness of the amorphous layer.

Contacts were deposited on the porous layer at a ~30° angle to eliminate penetration of the metal into the pores and short-circuiting of the layer. All electrophysical measurements were performed on the ohmic portion of the current-voltage characteristic, which corresponded to the ±200 mV voltage range.

The samples were prepared as detailed in Table I. The density deficiency of porous silicon (the porosity P) is usually determined by a gravimetric method. The sample is weighed before etching, after etching, and after removal of the porous layer in KOH. However this method requires large thicknesses of porous silicon (more than a micron) to achieve the required weighing accuracy. In our case the porous layers were thinner than 0.3 μ. As a result, the porosity was determined gravimetrically with a large error and had a value of $P = 50 \pm 20\%$ for samples Nos. 3–5. No mass change could be detected after anodic etching in sample No. 2. The value of P can be determined more accurately by measuring the dielectric constant ϵ in the effective-medium approximation,⁹ which has proved itself in the case of crystalline porous silicon.¹⁰ According to Ref. 9, P and ϵ are related by the expression

$$P(1 - \epsilon)/(1 + 2\epsilon) + (1 - P)(\epsilon_{\text{Si}} - \epsilon)/(\epsilon_{\text{Si}} + 2\epsilon) = 0,$$

where $\epsilon_{\text{Si}} = 12$ is the dielectric constant of compact *a*-Si. The value of ϵ was found by measuring the capacitance of the structures at 10²–10⁶ Hz and $T = 77$ K. It was taken into account that the capacitances of the porous and compact layers of *a*-Si were connected in series. The results obtained by this procedure are presented in Table I.

3. DYNAMIC CONDUCTIVITY

Information on the charge transfer mechanism in a disordered system is often obtained by measuring the dynamic conductivity. The electrical conductivity is measured as a function of the frequency ω of the alternating electric field. Also, the dynamic conductivity $\sigma_{\text{ac}}(\omega) = \sigma(\omega, T) - \sigma(0, T)$ should vary, depending on whether the charges move along extended states or jump between localized states. When carriers are excited through the mobility edge into the region of delocalized states, the conductivity does not depend on the frequency up to 10⁸ Hz. If conduction is mediated by

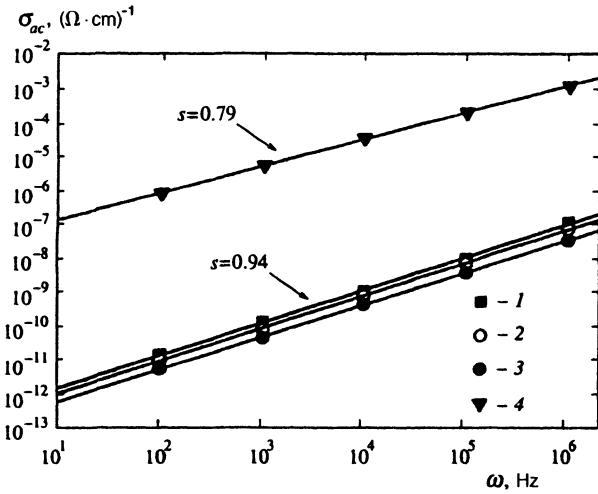


FIG. 2. Dependence of the dynamic conductivity on the frequency of the electric field for porous silicon sample No. 5 ($T=300$ (1), 230 (2), 130 (3) K) and for compact a -Si ($T=300$ K (4)).

phonon-stimulated hops between localized states, the conductivity should increase with the frequency according to a power law.

Dynamic conduction involving phonons is a relaxation mechanism, under which an electron passes from one level to another at a distance R by means of the absorption or emission of a phonon of frequency

$$\omega = \nu_0 \exp(-2R/a), \quad (1)$$

where ν_0 is the characteristic phonon frequency (in silicon it is of the order of 10^{12} – 10^{13} Hz). The electric field alters the equilibrium occupation numbers of the sites, causing relaxation to the equilibrium state specified by the instantaneous value of the field. There is a delay accompanied by the dissipation of energy. The optimum states for such transitions form compact pairs at a considerable distance from one another. There are no transitions between pairs, and thus they cannot participate in the static conduction, but a high-frequency field induces displacement currents. It is clear that states of both percolation and finite clusters take part in dynamic conduction.

Considering the situation in which hops occur between states near the Fermi level, Austin and Mott¹¹ obtained the expression

$$\sigma_{ac}(\omega) = \text{const} \cdot T \omega^s, \quad (2)$$

where the exponent s is a weak function of the frequency and is given in the three-dimensional case by the expression

$$s = 1 - 4 / \ln(\nu_0 / \omega). \quad (3)$$

In disordered and amorphous semiconductors we usually have $s \approx 0.8$.

Figure 2 presents the dependence of the conductivity on frequency for compact and porous a -Si (the etching time was 12 s). In the frequency range $\omega = 10^2$ – 10^6 Hz the law (2) is valid for both systems, with $s = 0.79 \pm 0.01$ for compact a -Si and $s = 0.94 \pm 0.01$ for the porous sample. We can use Eq. (3) to evaluate the characteristic phonon frequency. Taking $\omega = 10^4$ Hz and $s = 0.79$, we obtain $\nu_0 = 2 \times 10^{12}$ Hz. An

attempt to evaluate ν_0 using Eq. (3) in the case of porous silicon leads to the physically unreasonable value $\nu_0 \approx 5 \times 10^{30}$ Hz. In our opinion, this disparity stems from the fractal nature of the space filled by the silicon. According to Ref. 12, hopping conduction on fractals with a dimension D and a superlocalization exponent ζ in the wave functions should vary with frequency according to (2), where

$$s = 1 - \zeta^{-1} \frac{D + 2 - \zeta}{\ln(\nu_0 / \omega)}. \quad (4)$$

There are two theoretical models, which interpret ζ differently. One¹³ defines the superlocalization exponent as half the fractal dimension of the random walks $D_w = 3.8$ and is supported by experiments on carbon-black-polymer composites. The other¹⁵ identifies ζ with the dimension of the shortest path in a typical cluster $D_{\min} = 1.36$. Taking $\zeta = 1.9$ (Ref. 14), $\omega = 10^{2-6}$ Hz, and $\nu_0 = 2 \times 10^{12}$ Hz, from (4) we found that D lies in the range from 2.1 to 2.5. In the case of $\zeta = 1.36$ we obtained an underestimate: $D = 0.8$ – 1.2 .

4. ANOMALOUS CURRENT RELAXATION

The next unusual result of the present work is the observation of prolonged current relaxation after a voltage step is applied to the structure. The experiment consisted of applying a fixed bias $U_0 = 50$ mV to the sample at time $t_0 = 0$. This caused the appearance of an electric current $I(t)$ in the system, which decreased with the passage of time to its stationary value $I_s \equiv I(t = \infty)$. Figure 3a shows the relative variation of the current as a function of time $\Delta I(t)/I_s = [I(t) - I_s]/I_s$ for various layers of porous silicon at room temperature. It is noteworthy that similar relaxation of the conductivity of a metal-insulator-conductor channel in an In_2O_3 transistor was observed in Ref. 16 at $T = 4.2$ K after a gate voltage $U_g > 100$ V was applied and was attributed to nonequilibrium charge transport in the hopping regime.

In our opinion, the cause of the relaxation behavior is closely related to the appearance of dynamic conductivity at the moment when the electric field is turned on. We assume that a voltage is created at time t_0 and reaches its stationary value U_0 at time t_1 . Then, during the interval $\Delta t = t_1 - t_0$ the sample experiences a variable electric field, which results from the superposition of a large set of harmonic signals. Displacement currents appear in it in finite clusters, and an ordinary current appears in the percolation cluster. At times $t > t_1$ the displacement currents decay as a consequence of redistribution of the electrons among the sites, and a less conductive stationary state is established. In ordered systems relaxation is usually a Debye (normal) process and takes place within very short times, whose determination requires a special experimental setup. An analysis of the relaxation curves in porous amorphous silicon revealed the following.

1) The dependence $I(t)$ exhibits nonexponential behavior: it cannot be described by a single relaxation time; the dashed line in Fig. 3b is the result of fitting an exponential function to the experimental plot of $I(t)$ by the least-squares method, and the relaxation process cannot be described by a power function (Fig. 3b, dotted line).

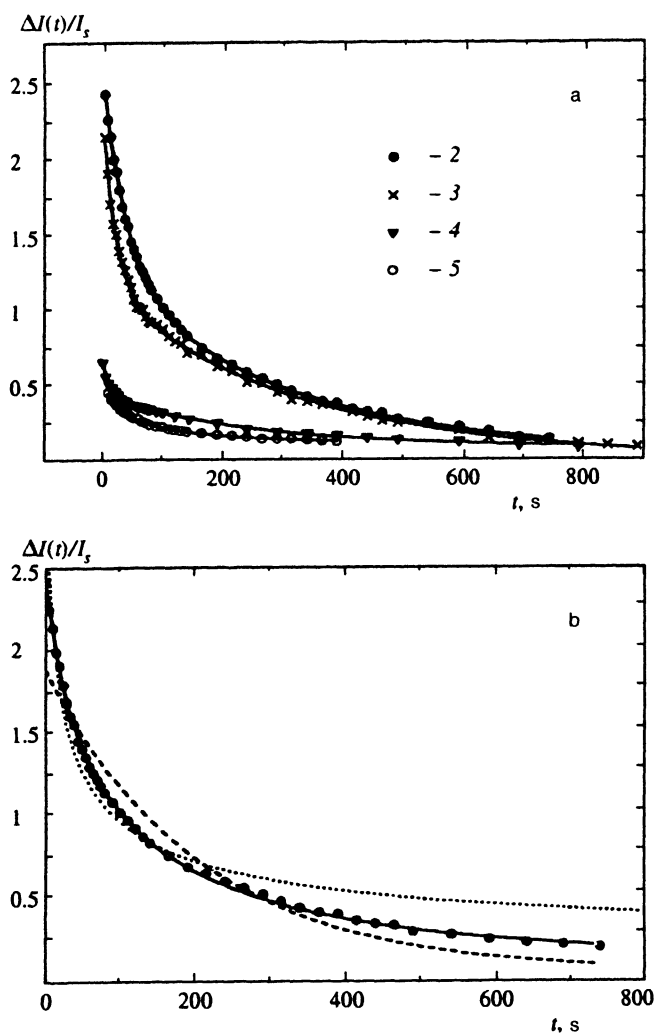


FIG. 3. a) Current decay kinetics after applying a 50-mV voltage step 50 mV to the structure. The numbered curves correspond to the numbered samples in Table I. b) Approximation of the current relaxation in sample No. 2 by the exponential function $A \exp(-t/t_0)$ (dashed curve) and by the power law $At^{-\alpha}$ (dotted curve).

2) The current decays over times significantly exceeding the Maxwell time, which equals 10^{-4} – 10^{-1} s in the present case.

The fact that dielectric relaxation is anomalous in many glasses and polymers has been known since about 1970.¹⁷ It was found that a protracted decay law describes diverse types of relaxation in many complex disordered materials: for example, the residual magnetization of spin glasses, luminescence decay in porous glasses,¹⁹ diffusion in porous materials, and processes occurring during the chromatographic separation of substances.²⁰ The kinetics of the decrease in the nonstationary photoconductivity in amorphous materials are also often anomalous²¹ in the sense that they are described by a power law, rather than an exponential law. However, the characteristic times of such processes are still very small (10^{-6} – 10^{-4} s). Several theories have been proposed to explain the protracted law: a) anomalous dispersion of the times of the events; 2) direct transfer on fractals; 3) dynamics with hierarchical constraints; and 4) diffusion with fractally distributed times. The common factor among these

models is the existence of a hierarchy of relaxation times, whose distribution is fairly broad. The strong spatial inhomogeneity inherent to all disordered media, which determines the distribution of the interatomic distances, makes the range of microscopic transition rates very broad. Thus, spatial disorder leads to temporal disorder. Clearly, the presence of superlocalization in porous silicon should significantly shift the distribution function of the transition times toward larger values, thereby drastically slowing the kinetics of various reactions.

The lack of a steady state in the electronic subsystem of porous silicon during the conduct of a real physical experiment attests to the nonergodicity of this system as a Fermi glass. The concept of a Fermi glass as applied to Anderson insulators has existed since Mott's pioneering work,²² but, many of the properties of disordered systems predicted on the basis of this model are still only scientific hypotheses. One of these properties is the nonergodicity of Fermi glasses. As we know, experimentally measured macroscopic parameters are averages over time, while the theory gives averages over a statistical ensemble of microstates that imitate the real states at different moments in time. In ergodic systems all the microstates are achievable during the course of a real physical experiment; therefore, the two types of averages can be considered identical. This permits the comparison of theoretically determined and experimentally observed macroscopic parameters. In nonergodic systems such a procedure is far from trivial. The concept of nonergodicity as applied to porous silicon must only be used to stipulate a restricted time interval ($t < 10^3$ s), within which ergodic behavior probably exists. This permits investigation of the temperature dependence of the static conductivity σ_{dc} after the system relaxes to a stationary state.

5. TEMPERATURE DEPENDENCE OF THE STATIC CONDUCTIVITY

Figure 4 presents the temperature dependence of the conductivity in Arrhenius coordinates after current relaxation for 30 min at room temperature. It is seen that the conductivity of the porous layers is significantly lower than the conductivity of compact *a*-Si and depends on the etching time (the porosity of the material). It is convenient to investigate the behavior of $\sigma_{dc}(T)$ by analyzing the local activation energy for conduction^{23,24} $W(T) = -d(\ln \sigma)/d(1/kT)$. Here we take advantage of the fact that the known laws describing the variation of $\sigma_{dc}(T)$ on the insulator side of an Anderson junction are special cases of the general expression

$$\sigma_{dc}(T) = \sigma_i \exp[-(T_i/T)^n], \quad (5)$$

where the exponent n is closely related to the dimensionality of the medium.

It is easily seen from (5) that

$$W(T) = n(kT_i)^n (kT)^{1-n}. \quad (6)$$

Figure 5 shows the temperature dependence of the activation energy obtained by direct differentiation of the experimental points for $\sigma_{dc}(T)$. Two hopping conduction regimes are realized for the porous layers: in the high-temperature range $250 < T < 300$ K the activation energy decreases mono-

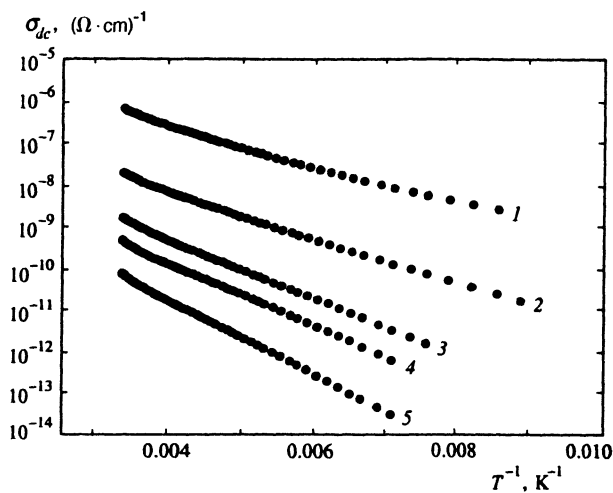


FIG. 4. Temperature dependence of the static conductivity in samples 1–5.

tonically with increasing temperature, and at low temperatures $W(T)$ scarcely depends on T . For compact a -Si the activation energy varies with the temperature over the entire range of T investigated. Table II presents fits to the experimental data on $\sigma_{dc}(T)$ using Eq. (7) in the high- (σ_0 , T_0 , and n) and low-temperature (σ_1 , T_1 , and n_1) ranges. In our preceding study¹ (see also the reference in footnote 1) the transition detected in porous a -Si_{1-x}Mn_x and a -Si obtained by ion implantation, from a conduction regime with variable activation energy to a regime with a constant value of W as the temperature decreases, can be ascribed to a change to one-dimensional electron trajectories as the hopping distance increases. Below we do not dwell in detail on one-dimensional transport, and we discuss only the behavior of the conductivity at high temperatures.

Several hopping conduction mechanisms that lead to different values of the exponent n have been described in the literature:

- (1) $n = 1/(D + 1)$ — the familiar Mott law in the absence of Coulomb correlations²⁵;
- (2) $n = 1$ for one-dimensional hopping conduction^{26–28};
- (3) $n = \zeta/(D + \zeta)$ for charge transfer along fractals between states with a superlocalized wave function.¹³

Using the expression $n = 1/(D + 1)$, we find that $D = 3.00 \pm 0.25$ for compact a -Si and $D = 3.15 \pm 0.27$ for porous silicon with porosity 37%. Therefore, in these samples the dimensionality of the space responsible for transport of the static current is Euclidean. This makes it possible to use the familiar relation for Mott's law $kT_0 = 16g_3a^3$ to determine the three-dimensional density of states g_3 . Taking $T_0 = 5 \times 10^7$ K for sample 1 and $T_0 = 8 \times 10^7$ K for sample 2,

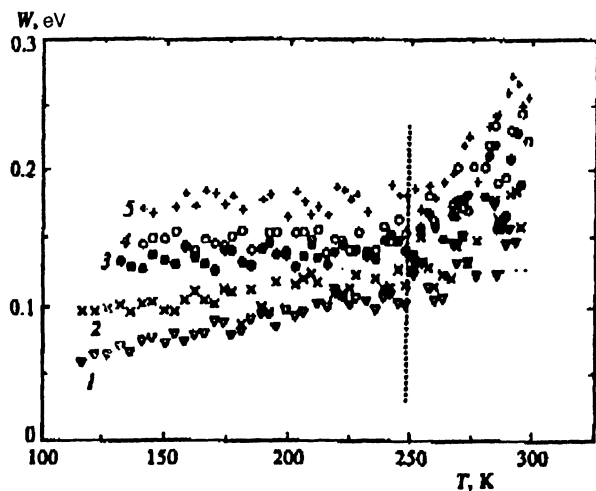


FIG. 5. Temperature dependence of the activation energy for conduction obtained by direct differentiation of the experimental dependence of $\sigma_{dc}(T)$ in samples 1–5.

we obtain $g_3 = 1.36 \times 10^{20} \text{ eV}^{-1} \cdot \text{cm}^{-3}$ and $g_3 = 8.5 \times 10^{19} \text{ eV}^{-1} \cdot \text{cm}^{-3}$, respectively. An attempt to determine the dimensionality of the system in structures with high porosity from Mott's law leads to the clearly underestimated result $D = 1.17 \pm 0.06$ to 1.22 ± 0.06 for $n = 0.45 \pm 0.02$ to 0.46 ± 0.02 . In order for the procedure for evaluating D to be correct in this case, the details of the localization of the wave functions on the fractals must be taken into account, as in the analysis of the dynamic conductivity. Taking $\zeta = 1.9$ and using the formula $n = \zeta/(D + \zeta)$, we obtain $D = 2.23 \pm 0.10$ to 2.32 ± 0.10 (see Table II).

The appropriateness of the fractal conduction mechanism used to interpret the experimental data can be tested by evaluating the superlocalization radius a_s and the typical hopping distance over the percolation cluster R_l . The two-sided inequality

$$R_l(T) > R_0 > a_s \quad (7)$$

should hold.

The first condition is necessary for the hopping conduction mechanism with variable hopping distance, and the second is necessary for superlocalization when electrons tunnel between sites.

To evaluate a_s , we utilize the relation between T_0 and a_s found in Ref. 13:

$$kT_0 \approx [g_3 l_0^3 (a_s / l_0)^D]^{-1}, \quad (8)$$

where l_0 is the minimum scale on the basis of which a fractal medium can be constructed. It is natural to take the mean

TABLE II. Parameters of the temperature dependence of the static conductivity.

| No. | $\sigma_0 \times 10^3, \Omega^{-1} \cdot \text{cm}^{-1}$ | T_0, K | n | D | $\sigma_1, \Omega^{-1} \cdot \text{cm}^{-1}$ | T_1, K | n_1 |
|-----|--|-------------------------------|-----------------|-----------------|--|-----------------|-----------------|
| 1 | 83000 ± 4100 | $(5.07 \pm 0.04) \times 10^7$ | 0.25 ± 0.02 | 3.00 ± 0.30 | — | — | — |
| 2 | 81 ± 13 | $(8.07 \pm 0.02) \times 10^7$ | 0.24 ± 0.02 | 3.15 ± 0.27 | $(1.8 \pm 0.1) \times 10^{-6}$ | 2430 ± 353 | 0.81 ± 0.03 |
| 3 | 3.2 ± 0.5 | $(1.25 \pm 0.02) \times 10^5$ | 0.45 ± 0.02 | 2.32 ± 0.12 | $(3.9 \pm 0.1) \times 10^{-7}$ | 2353 ± 60 | 0.89 ± 0.02 |
| 4 | 1.7 ± 0.4 | $(1.00 \pm 0.05) \times 10^5$ | 0.46 ± 0.02 | 2.23 ± 0.10 | $(1.44 \pm 0.05) \times 10^{-7}$ | 1995 ± 70 | 0.96 ± 0.04 |
| 5 | 3.7 ± 0.7 | $(1.34 \pm 0.03) \times 10^5$ | 0.46 ± 0.02 | 2.23 ± 0.10 | $(5.4 \pm 2.1) \times 10^{-8}$ | 2016 ± 253 | 0.99 ± 0.04 |

distance between silicon atoms, which equals 0.27 nm, as l_0 . The value of T_0 for porous silicon with fractal conduction (samples Nos. 3–5) equals 1.0×10^5 to 1.3×10^5 K. Using this value, as well as $D = 2.23$ – 2.32 and $\zeta = 1.9$, from (8) we obtain $a_s \approx 1.1$ nm. The typical hopping distance found with the optimization procedure in Ref. 13

$$R_i(T) \approx a_s (T_0/T)^{1/(D+\zeta)}. \quad (9)$$

Then $R_i(T) \approx 5.2 \cdot (300/T[\text{K}])^{0.46}$ nm, and the inequalities (7) do, in fact, hold.

6. CONCLUSIONS

In closing, we compare the values of the fractal dimensionality of the medium D derived from different experiments. Analyses of the frequency dependence of the dynamic conductivity and the temperature dependence of the static conductivity in porous silicon give approximately the same value of D , which depends only on the porosity of the material. This is a convincing argument favoring a single approach to the various electrophysical phenomena based on the idea of a fractal space.

It is noteworthy that fractal topology produces the most distinctive consequences specifically in porous amorphous silicon, i.e., a material in which hopping conduction is the dominant mechanism of current transfer. It is known that the self-similarity of porous silicon exists only in a restricted range of scales L : $l_0 < L < \xi$. According to the data in Refs. 2 and 4, the correlation length ξ can have a value of the order of 100 nm. On scales $L > \xi$ the system behaves as a homogeneous semiconductor with a dimensionality equal to the Euclidean value. The hopping distance R , which amounts to several nanometers, serves as the characteristic scale on which hopping conduction occurs as a physical phenomenon. The fact that $l_0 < R < \xi$ also makes hopping transport have fractal properties.

This work was performed with financial support from the International Science Foundation (Grant No. U88300), the ‘‘Physics of Solid-State Nanostructures’’ State Program (Grant No. U88300), and the international association INTAS (Grant No. 94-4435). We thank V. I. Obodnikov and A. M. Myasnikov for recording the SIMS spectra, and É. M. Gaskin for a useful discussion of the results.

¹⁾A. I. Yakimov, A. V. Dvurechenskii, N. P. Stepina, *et al.* (in press).

- ¹A. I. Yakimov, N. P. Stepina, A. V. Dvurechenskii, and L. A. Scherbakova, *Physica B (Amsterdam)* **205**, 298 (1995).
- ²M. Ben-Chorin, F. Moller, F. Koch *et al.*, *Phys. Rev. B* **51**, 2199 (1995).
- ³P. Goudeau, A. Naudon, G. Bomchil, and R. Herino, *J. Appl. Phys.* **66**, 625 (1989).
- ⁴V. Vezin, P. Goudeau, A. Naudon *et al.*, *Appl. Phys. Lett.* **60**, 2625 (1992).
- ⁵B. J. Heuser, S. Spooner, C. J. Glinka *et al.*, *Mater. Res. Soc. Symp. Proc.* **283**, 209 (1993).
- ⁶R. L. Smith and S. D. Collins, *J. Appl. Phys.* **71**, R1 (1992).
- ⁷Y.-E. Lévy and B. Souillard, *Europhys. Lett.* **4**, 233 (1987).
- ⁸R. Herino, G. Bomchil, K. Barla *et al.*, *J. Electrochem. Soc.* **134**, 1994 (1987).
- ⁹D. E. Aspnes, J. B. Theeten, and F. Hottier, *Phys. Rev. B* **20**, 3293 (1979).
- ¹⁰P. A. Badoz, D. Bensahel, G. Bomchil *et al.*, *Mater. Res. Soc. Symp. Proc.* **283**, 97 (1993).
- ¹¹L. G. Austin and N. F. Mott, *Adv. Phys.* **18**, 41 (1969).
- ¹²Xiao-Bing Wang, Qing Jiang, Zhe-Hua Zhang, and De-Cheng Tian, *J. Phys.: Condens. Matter* **7**, 3279 (1995).
- ¹³G. Deutscher, Y.-E. Lévy, and B. Souillard, *Europhys. Lett.* **4**, 577 (1987).
- ¹⁴D. van der Putten, J. T. Moonen, H. B. Brom *et al.*, *Phys. Rev. Lett.* **69**, 494 (1992).
- ¹⁵A. Aharony and A. Brooks Harris, *Physica A (Amsterdam)* **163**, 38 (1990).
- ¹⁶M. Ben-Chorin, Z. Ovadyahu, and M. Pollak, *Phys. Rev. B* **48**, 15 025 (1993).
- ¹⁷G. Williams and D. C. Watts, *Trans. Faraday Soc.* **66**, 80 (1970).
- ¹⁸R. V. Chamberlin, G. Mazurkewich, and R. Orbach, *Phys. Rev. Lett.* **52**, 867 (1984).
- ¹⁹U. Even, K. Rademann, J. Jortner *et al.*, *Phys. Rev. Lett.* **52**, 2164 (1984).
- ²⁰G. H. Weiss, *Sep. Sci.* **5**, 51 (1970).
- ²¹H. Scher and E. W. Montroll, *Phys. Rev. B* **12**, 2455 (1975).
- ²²N. F. Mott and E. A. Davis, *Electronic Processes in Non-Crystalline Materials*, 2nd ed. Clarendon Press, Oxford (1979).
- ²³A. G. Zabrodskii and I. S. Shlimak, *Fiz. Tekh. Poluprovodn.* **9**, 587 (1975).
- ²⁴R. M. Hill, in *Proceedings of the 7th International Conference on Amorphous and Liquid Semiconductors*, W. E. Spear (ed.) University of Edinburgh, Edinburgh (1977), p. 229.
- ²⁵N. F. Mott, *Philos. Mag.* **19**, 835 (1969).
- ²⁶J. Kurkijarvi, *Phys. Rev. B* **8**, 922 (1973).
- ²⁷M. E. Raikh and I. M. Ruzin, *Zh. Éksp. Teor. Fiz.* **95**, 1113 (1989) [*Sov. Phys. JETP* **68**, 642 (1989)].
- ²⁸I. P. Zvyagin, *Zh. Éksp. Teor. Fiz.* **107**, 175 (1995) [*JETP* **80**, 93 (1995)].

Translated by P. Shelnitz